Epitaxial growth of gadolinium oxide on roll-textured nickel using a solution growth technique

Jonathan S. Morrell and Ziling B. Xue
Department of Chemistry, University of Tennessee, Knoxville, Tennessee 37996

Eliot D. Specht, Amit Goyal, Patrick M. Martin, and Dominic F. Lee
Metals and Ceramics Division, Oak Ridge National Laboratory, Oak Ridge, Tennessee 37831

R. Feenstra, D.T. Verebelyi, and D.K. Christen
Solid State Division, Oak Ridge National Laboratory, Oak Ridge, Tennessee 37831

Thomas G. Chirayil, Mariappan Paranthaman, Catherine E. Vallet, and David B. Beach[a)]
Chemical and Analytical Sciences Division, Oak Ridge National Laboratory, Oak Ridge, Tennessee 37831

(Received 2 August 1999; accepted 20 December 1999)

Chemical solution epitaxy was used to deposit an epitaxial film of Gd_2O_3 on roll-textured nickel. A 2-methoxyethanol solution of gadolinium methoxyethoxide was used for spin-coating and dip-coating. Films were crystallized using a heat treatment at 1160 °C for 1 h in 4% H_2/96% Ar. Single-layer films were approximately 600 Å in thickness, and thicker films could be produced using multiple coatings. $\theta/2\theta$ x-ray diffractograms revealed only (004l) reflections, indicating a high degree of out-of-plane texture. A pole-figure about the Gd_2O_3 (222) reflection indicated a single in-plane epitaxy. Scanning electron microscopy showed that the films were smooth, continuous, and free of pin holes. Atomic force microscopy revealed an average surface roughness of 53 Å. Electron diffraction indicated that the misalignment of the majority of the grains in the plane was less than 10°. High-current (0.4 MA/cm^2) $YBa_2Cu_3O_{7-\delta}$ films were grown on roll-textured nickel substrates using Gd_2O_3 as the base layer in a three-layer buffer structure.

I. INTRODUCTION

The next generation of superconducting wire operating at liquid-nitrogen temperature (77 K) is predicted to use a "coated conductor" architecture consisting of a polycrystalline copper oxide superconductor deposited on a mechanically robust metal tape.[1] In order to achieve high critical currents in copper oxide superconducting polycrystalline films, it is necessary to have both good out-of-plane alignment (*c*-axis texture, ensuring that the Cu–O planes lie parallel to the substrate) and good in-plane alignment (avoiding "weak link" conduction between grains).[2] To achieve this alignment in practical coated conductors, two distinctly different approaches to inexpensive substrates are being pursued. One approach involves the deposition of a textured buffer layer on a randomly oriented, oxidation resistant metal tape using multiple ion beams in a technique known as ion beam assisted deposition (IBAD).[3] The other approach involves the deposition of an epitaxial buffer layer on a roll-textured metal tape in a technique known as rolling-assisted biaxially textured substrates (RABiTS).[4]

The first successful RABiTS buffer layer architecture used laser ablation to deposit an epitaxial layer of palladium on roll-textured nickel, followed by a layer of cerium oxide and a layer of yttrium-stabilized zirconia (YSZ).[5] Later RABiTS architectures dispensed with the palladium layer.[6] As an alternative to pulsed laser ablation, e-beam evaporation and sputtering have also been used to deposit ceramic layers.[7] The best results to date use a thin (500 Å) cerium oxide layer in contact with the nickel, a fairly thick (5000 Å) YSZ layer, and a thin cap layer of (500 Å) cerium oxide. Recently, buffer layers using rare-earth oxides deposited by physical vapor deposition have been shown to also give high critical currents.[8,9] As an alternative to the relatively higher cost and complexity of vacuum deposition techniques, we have been examining solution routes to epitaxial films on roll-textured nickel. We have previously reported on epitaxial growth of $LaAlO_3$, $NdAlO_3$, and $PrAlO_3$.[10,11] In each of these cases, we were unable to obtain solely the desired [001]||[001] cube-on-cube epitaxy but rather a

[a)]Address all correspondence to this author.

 © 2000 Materials Research Society

mixture of predominantly (~70%) cube texture with a 45° rotated [001]‖[011] epitaxy. In this paper, we report the deposition of Gd_2O_3 on roll-textured nickel to give a single epitaxy. These buffered substrates may provide a low-cost substrate for copper oxide superconductor deposition.

II. EXPERIMENTAL

All solution manipulations were carried out under an atmosphere of argon using standard Schlenk techniques. Gadolinium metal and 2-methoxyethanol (Alfa) were used as received and 2-propanol was dried by distillation from aluminum isopropoxide. Gadolinium isopropoxide was prepared from gadolinium metal and dry 2-propanol in the presence of a mercury salt catalyst by the method of Brown and Mazidiyansi.[12] Because it is not possible to purify gadolinium methoxyethoxide (a viscous, nonvolatile oil) by either recrystallization or distillation, it was essential to start with very pure gadolinium isopropoxide. The initial reaction mixture was purified by passage down a short column of Celite in a Schlenk filter. The solvent (2-propanol) was removed, and the residue was extracted using a Soxhlet extractor using dry 2-propanol. On cooling, colorless crystals of gadolinium isopropoxide were obtained. The infrared (IR) spectra were in excellent agreement with the literature.[12]

A gadolinium methoxyethoxide solution in 2-methoxyethanol was prepared by charging a flask with 4.18 g of gadolinium isopropoxide and 50 ml of 2-methoxyethanol. The flask was refluxed for 1 h, and 35 ml of solvent (2-propanol and 2-methoxyethanol) was removed by distillation. The contents were rediluted with additional 2-methoxyethanol, and the distillation/redilution cycle was repeated twice more to completely exchange the isopropoxide ligand for the methoxyethoxide ligand. The final concentration was adjusted to produce 50 ml of a 0.25 M stock solution. (When protected from the atmosphere, this solution is stable for more than 1 year). Four parts of the stock solution was mixed with one part 1.0 M H_2O in 2-methoxyethanol to produce a coating solution. These partially hydrolyzed coating solutions will reproducibly prepare high-quality coatings for several days to several weeks.

Mechanically deformed nickel was ultrasonically cleaned with dry 2-propanol for 1 h to free the nickel surface of oil from the roller. The cleaned nickel was subjected to a heat treatment at 700 °C in an atmosphere of 4% H_2/96% Ar for 1 h to develop the cubic texture. (Details of the roll-texturing process are described elsewhere.[5]) Both spin-coating and dip-coating techniques were used to coat the nickel substrates. For spin coating,

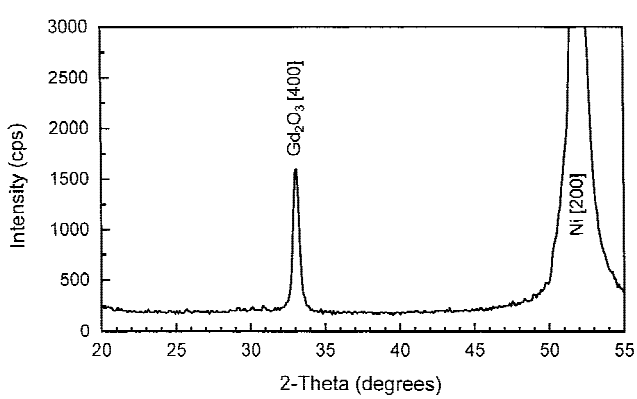

FIG. 1. θ/2θ x-ray diffratogram of an 600-Å Gd_2O_3 film on roll-textured nickel showing both excellent texturing of the nickel substrate and the film.

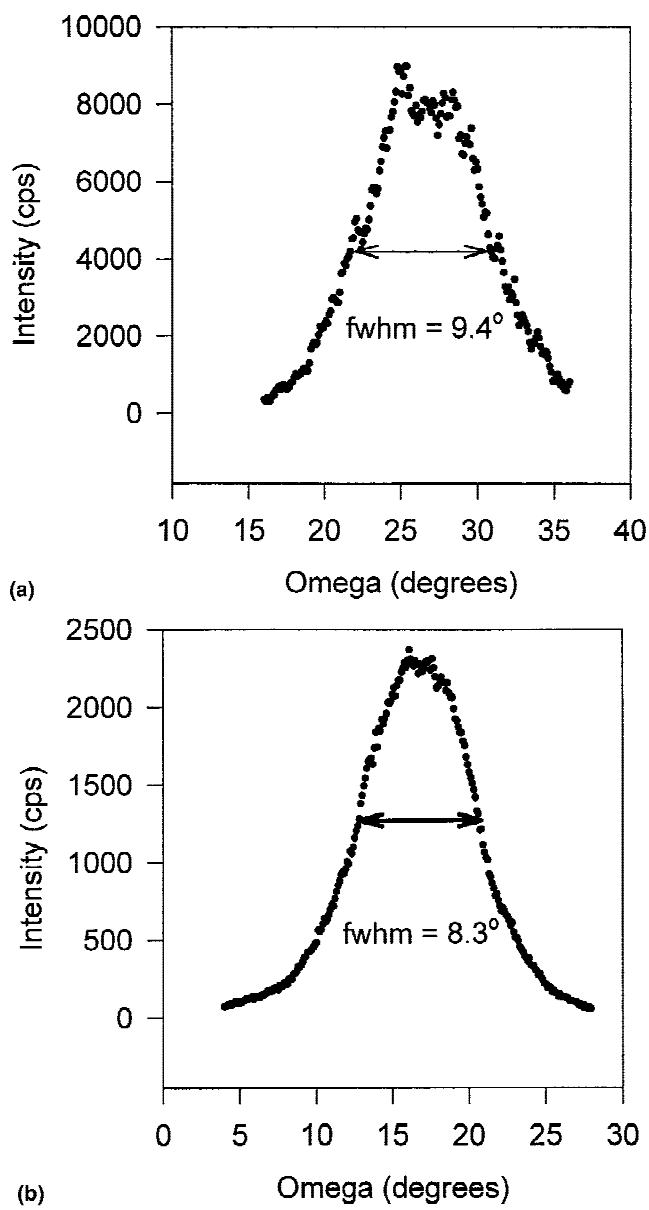

FIG. 2. Rocking curves (ω-scan) of the (a) Ni [200] and (b) Gd_2O_3 [400] reflections.

10 × 10 mm coupons were flooded with the solution and the excess solution was thrown-off by spinning for 45 s at 2000 rpm. Coated substrates were placed in a quartz tube equipped with a gas inlet and bubbler outlet and were purged for 15 min at room temperature using 4% H_2/96% Ar. The tube was then placed in a preheated tube furnace and held at 1160 °C for 1 h. Films are typically 600 Å [as measured using profilometry and Rutherford backscattering spectroscopy (RBS)] in thickness after firing, and multiple coatings could be used to prepare thicker films. For dip coating, strips of nickel, typically 10 × 60 mm, were immersed in the coating solution and withdrawn mechanically at a rate of 3 cm/min. Coatings produced under these conditions were typically 500 Å in thickness after firing, and again, thicker layers could be produced by multiple coatings.

III. RESULTS

A. X-ray diffraction

Our principal tool for determining the structure of thin films is x-ray diffraction. A typical θ-2θ scan is shown in Fig. 1. The relative intensity of [004] reflection (33.1°) versus the [222] reflection (28.6°) is indicative of a high degree of *c*-axis orientation. [A randomly oriented

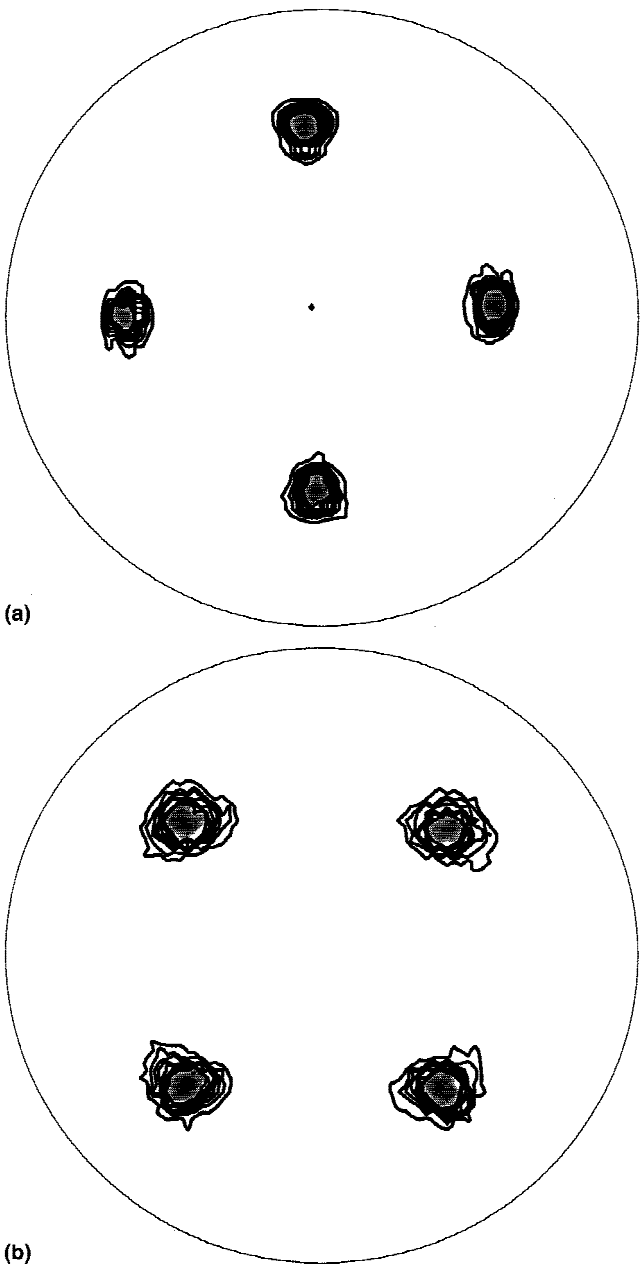

FIG. 3. Pole figures about the (a) Ni [111] and (b) Gd_2O_3 [222] planes of an 600-Å Gd_2O_3 film on roll-textured nickel.

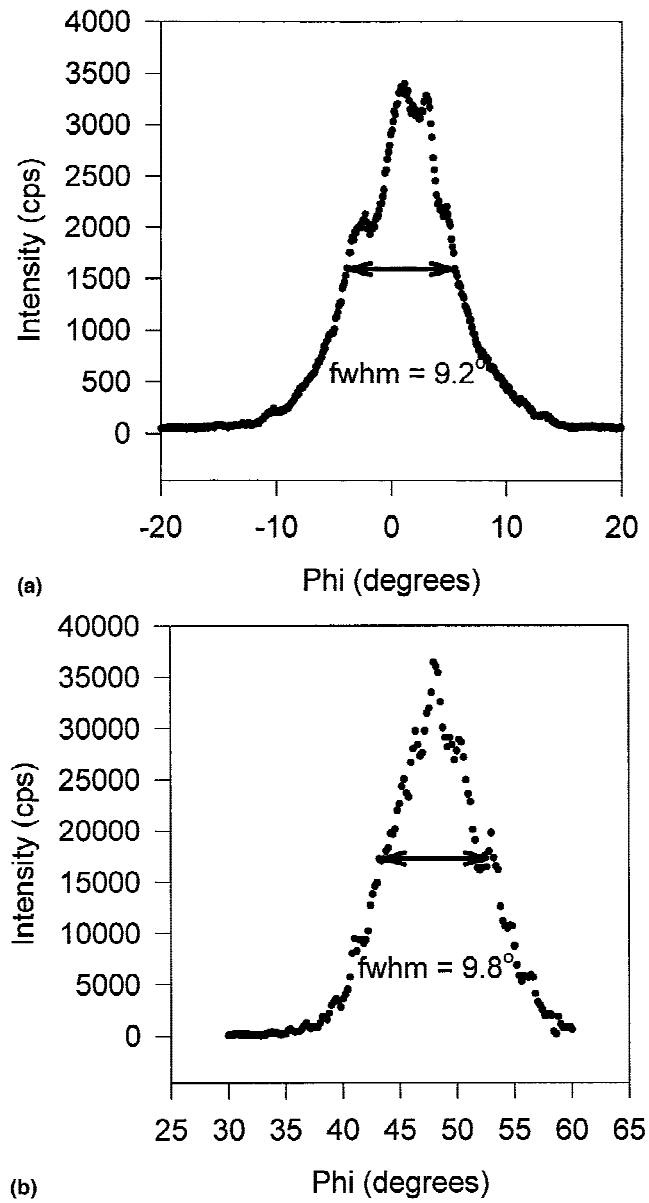

FIG. 4. Phi scans about the (a) Ni [111] and (b) Gd_2O_3 [222] planes of an 600-Å Gd_2O_3 film on roll-textured nickel.

film would have an intensity ratio ($I_{[222]}$ to $I_{[400]}$) of 100 to 30.[13]] Figure 2 shows rocking curves of the Ni [200] and Gd_2O_3 [400] reflections of this film. The full width at half-maximum (FWHM) of the film rocking curve is essentially the same as the roll-textured nickel. Although these peaks width are typically 2 orders of magnitude larger than those encountered in single crystals, they indicate a degree of alignment sufficient for the deposition of superconducting films with high critical currents.[2] In order to determine whether the film was aligned in-plane, pole figures about the film [222] plane and the substrate [111] plane were obtained (Fig. 3). The pole figures clearly indicate a $Gd_2O_3(110)\|Ni(100)$ epitaxial relationship between the film and the substrate. To quantitatively access the quality of the in-plane alignment, phi scans were obtained of both the film and the substrate (Fig. 4). Once again, the FWHM of the phi scans is large in comparison to single crystals but is comparable to the FWHM of RABiTS substrates that have been used to produce high-J_c superconducting films.

As mentioned earlier, thicker coatings could be produced by multiple coatings. Figure 5 shows θ-2θ scans of one to four layer coatings. The x-ray intensity of the (400) reflection increased with each successive coat, as did the intensity of the (222) and (321) reflections. In addition, a peak characteristic of the hexagonal phase was observed at 2θ of 30.1°. To rule out longer annealing time as the source of these changes in the diffraction pattern, several single-coat films were annealed for 15 min, 30 min, 1 h, 2 h, and 4 h at 1160 °C. Maximum x-ray intensity occurred at 1 h, with no change in either the (400) intensity or the (222) to (400) intensity ratio.

B. Film structure

Low-magnification scanning electron micrographs (SEM, Fig. 6) revealed a film morphology very similar to that of the nickel substrates. Tightly packed grains approximately 25 μm across were clearly observed. Higher magnification (Fig. 7) reveals a dense and continuous buffer layer. The images also clearly showed rolling marks on the nickel surface which have been conformally covered by the buffer layer. Although this film was not produced in a dust-free environment, relatively few pin holes or defects are observed.

Atomic force microscopy (AFM) was used to examine smaller areas, typically less than 10 × 10 μm, of a Ni

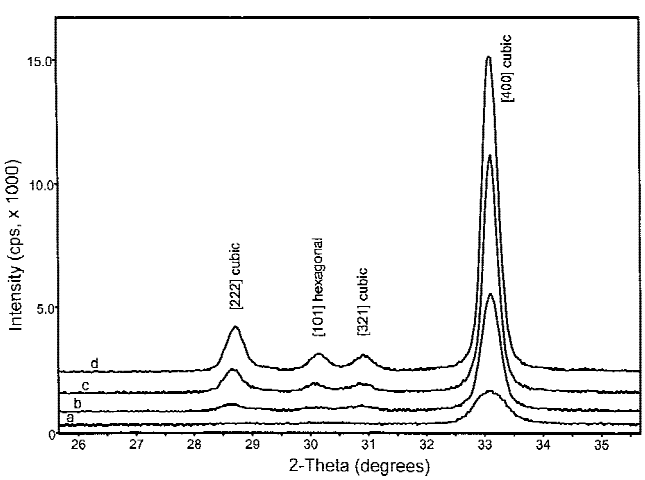

FIG. 5. θ/2θ x-ray diffratograms of 1 to 4 layer Gd_2O_3 films on roll-textured nickel.

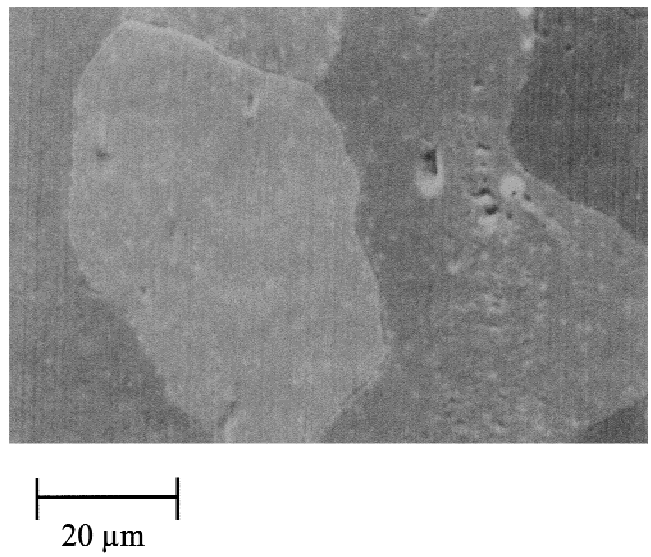

FIG. 6. Low-resolution backscattered SEM showing the large grain structure of the Gd_2O_3 film.

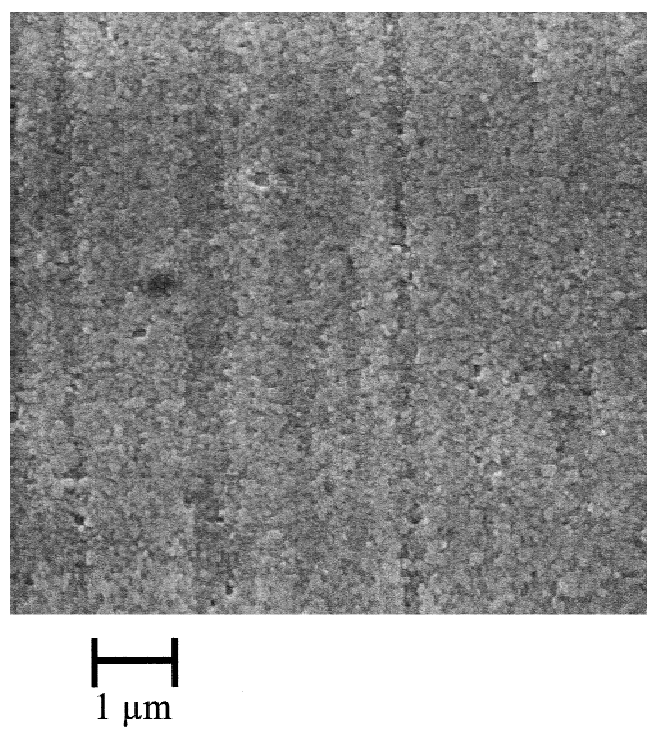

FIG. 7. High-resolution SEM showing surface structure.

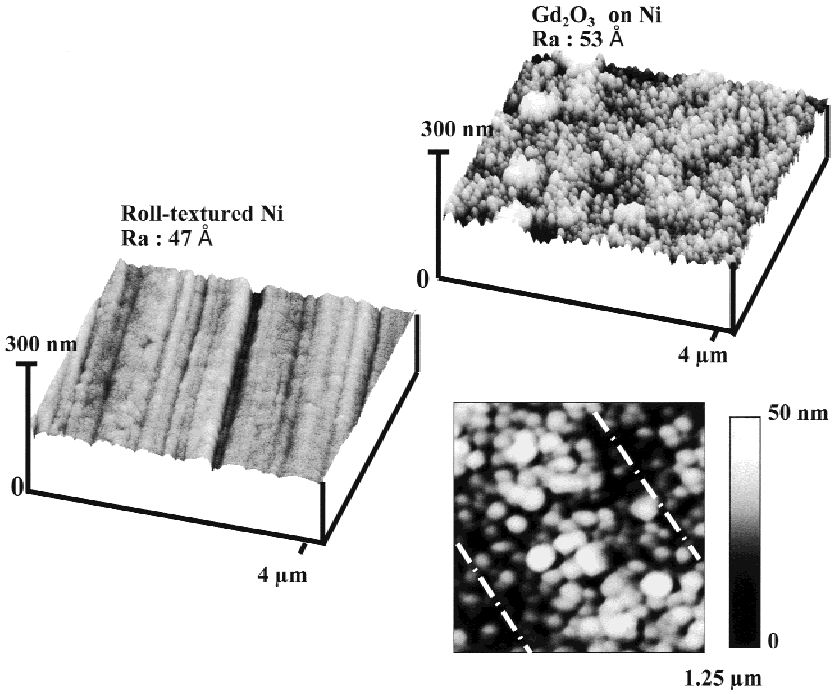

FIG. 8. Atomic force micrograph (AFM) of the surfaces of an annealed roll-textured nickel substrate and of a 600-Å Gd_2O_3 film deposited on roll-textured nickel (4 × 4 μm, $Z = 300$ nm). The 2D image is a zoom of Gd_2O_3 surface (1.25 × 1.25 μm, $Z = 50$ nm).

tape and of a Ni tape covered by one Gd_2O_3 layer. The images were obtained with a Nanoscope III and Si_3N_4 cantilevers in the contact mode. Figure 8 shows the 3D images of 4 × 4 μm areas of Ni tape and of a tape covered by a Gd_2O_3 layer. In addition, a (Gd_2O_3) 2D image of a smaller area (1.25 × 1.25 μm) is placed in the bottom right corner. The AFM image of the Ni tape shows parallel striations that may have been formed during the rolling process. The mean roughness (on the 16 μm^2 area), that is the mean value of the surface relative to the center plane, is 47 Å. The surface of the Gd_2O_3 layer has a different texture resulting from a compact assembly of near spherical grains. The 2D image suggests that the grains are arranged along lines of equal height from the zero-level. The two underlined dark regions correspond to recesses of the surface separated by a protuberant (i.e., light) area. The mean roughness calculated on a 4 × 4 μm area is 53 Å that is slightly larger than that of the Ni substrate. A more detailed analysis of the surfaces can be made by measuring the surface profiles along a direction perpendicular to the grooves of Ni surface or to the direction indicated in the Gd_2O_3 image. Figure 9 shows the resulting profiles that have obtained without averaging. From the surface profile of the Gd_2O_3 film (shown in the upper part of Fig. 9) particles appear fairly regular in size with diameter of about 100 nm. The nickel surface (shown in the lower part of Fig. 9) is smoother but shows striation with a depth of about 25 nm. It is interesting to point out that the difference in height between the protuberant Gd_2O_3 particles (in the center of the profile) and those in the recesses of the surface is also in the order of 25 nm. This observation suggests that the sol-gel film is formed by conformally covering the Ni surface.

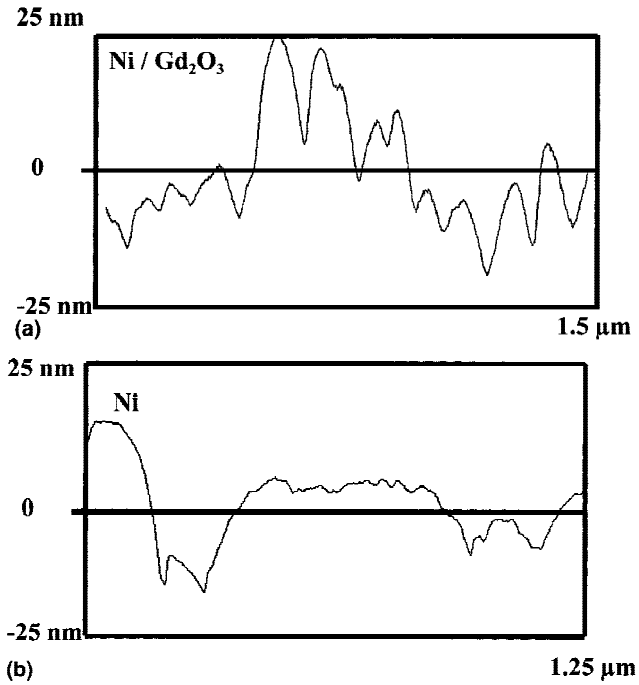

FIG. 9. Surface profiles of (a) Ni/Gd_2O_3 and (b) roll-textured nickel.

The effect of surface roughness and morphology on the deposition of subsequent layers is currently under investigation.

C. Electron diffraction

While x-ray diffraction is an excellent tool for the determination of bulk structure, the penetration depth of x-rays rendering the technique relatively surface insensitive. On the other hand, the diffraction of electrons provides an excellent probe of surface structure and grain alignment, two factors of critical importance for the production of high-J_c superconducting films. Backscattered Kikuchi diffraction was used to confirm the orientation of the Gd_2O_3 surface and to obtain a "map" of the orientation of individual grains. The details of this technique have been published in detail elsewhere.[14]

Figure 10 shows a set of pole figures constructed from the electron diffraction pattern. The results were identical to those obtained by x-ray diffraction in that only a single in-plane orientation was observed. This implies that the surface is highly textured, a necessary requirement for the deposition of high-J_c films. By the scanning of an area 100 × 100 μm, a map of grain orientation can be generated. Figures 11(a)–11(c) show misorientation of individual grains at the level of 1°, 5°, and 10°. The data clearly show that, at a misorientation of 10°, a percolative path for current exists.

D. Superconducting layer

Initial attempts to deposit $YBa_2Cu_3O_{7-\delta}$ (YBCO) using e-beam evaporated yttrium, barium fluoride, and copper followed *ex situ* heat treatment in water/oxygen[15] directly on sol-gel Gd_2O_3 buffered nickel were unsuccessful. The T_c of these films was ~80 K, the critical current (J_c) was low, and the x-ray diffraction of these films showed peaks characteristic of nickel oxide. The combination of lowered T_c and the presence of nickel oxide suggests that the films are not a good barrier to the diffusion of nickel from the substrate into the superconducting film. This may be due to several factors includ-

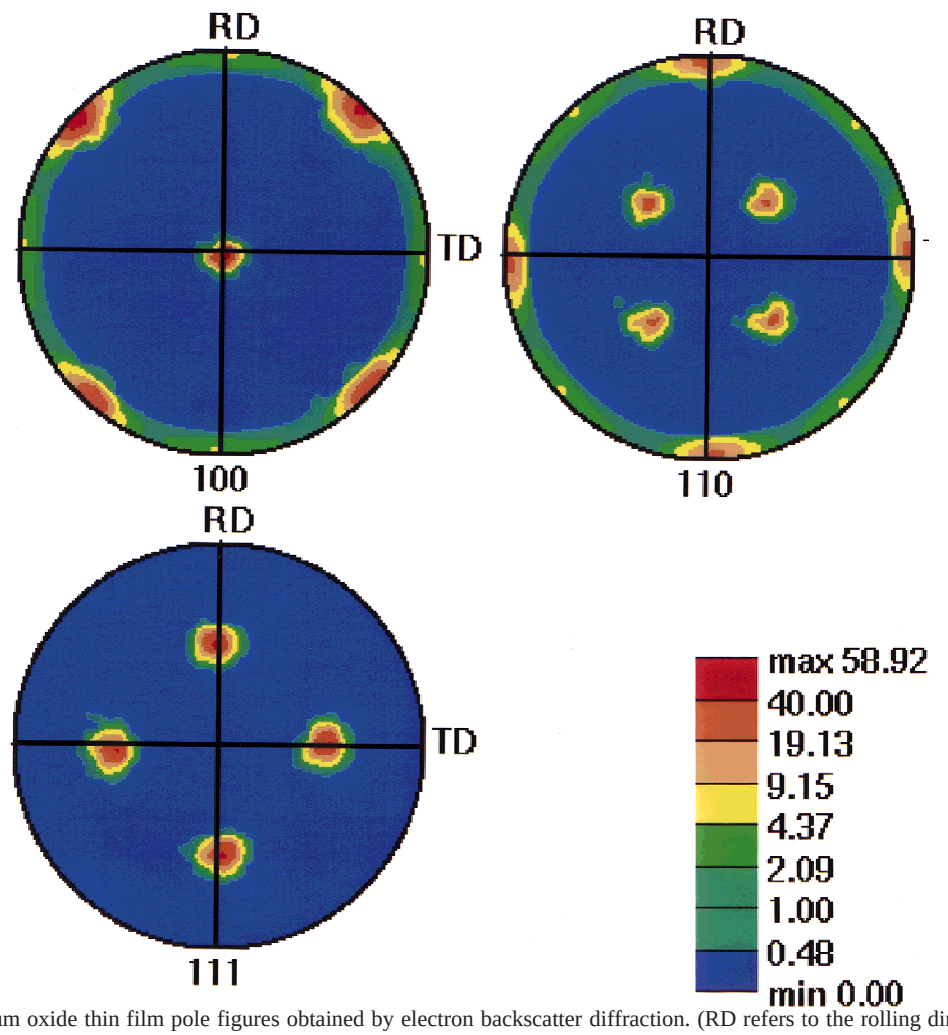

FIG. 10. Gadolinium oxide thin film pole figures obtained by electron backscatter diffraction. (RD refers to the rolling direction, and TD refers to the transverse direction.)

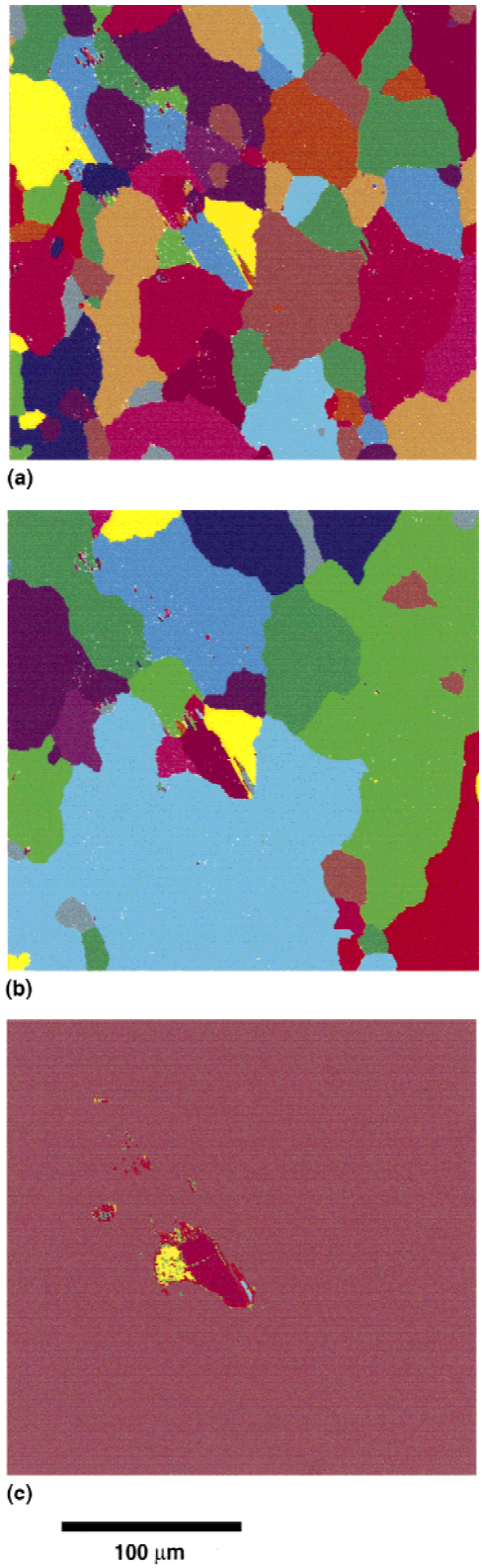

FIG. 11. Electron backscatter diffraction patterns of Gd_2O_3 on nickel showing grain misorientation. Color has been added to indicate a difference in in-plane grain alignment. Key: (a) grain misorientation less than 1%, (b) grain misorientation less than 5%, and (c) grain misorientation less than 10%.

ing porosity in the buffer layer or reaction of the buffer layer with the YBCO layer. We are currently investigating both improvements to the Gd_2O_3 buffer layer (better coverage, greater thickness, and "cap layers" such as cerium oxide) and other methods of YBCO deposition such as pulsed laser deposition (PLD).

To demonstrate that a sol-gel-synthesized Gd_2O_3 films may act as a template for further growth of epitaxial films, we have used Gd_2O_3-coated roll-textured nickel as the base for a high-critical current YBCO layer. In our "standard" RABiTS process, a thin (>500 Å) CeO_2 layer is deposited on the Ni, followed by a 0.5-μm-thick yttrium-stabilized zirconium oxide layer and capped by another thin CeO_2 layer. For this demonstration, we dip coated a 500-Å Gd_2O_3 layer on nickel which had been cleaned ultrasonically in dry 2-propanol as described in Sec. II. The coated substrate was heat treated at 1160 °C in flowing 4% H_2/96% Ar for 1 h. Without any further cleaning, we sputter deposited 0.5 μm of YSZ, followed by a cap layer of 500 Å of CeO_2. A 0.5-μm YBCO film was then deposited using the e-beam evaporated barium fluoride process described above.[15] Silver contacts were evaporated on to the sample for electrical measurements. A plot of resistivity versus temperature is shown in Fig. 12. This film has a T_c of 89 K and a critical current of 0.4 MA/cm^2. The value of critical current is within a factor of 3 of the results we typically obtain with a cerium oxide buffer layer deposited by physical deposition techniques.

IV. CONCLUSIONS

We have demonstrated that a solution technique can be used to obtain a single epitaxy on a roll-textured substrate. Considerable improvement to this process will be

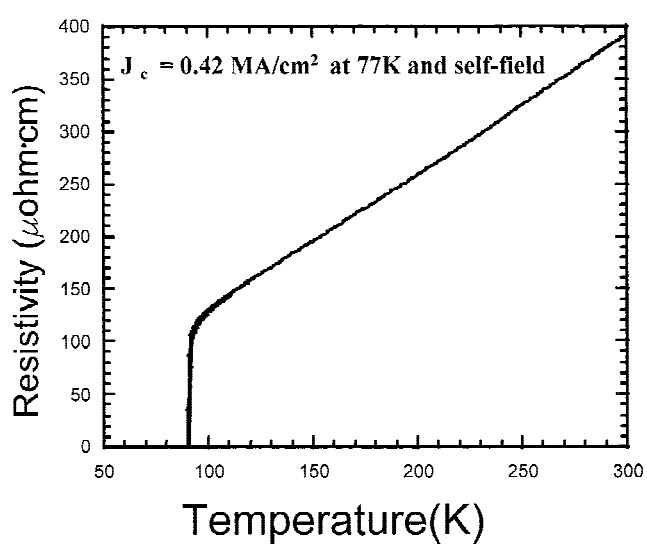

FIG. 12. Plot of resistivity versus temperature for a YBCO film deposited on a layered substrate consisting of roll-textured Ni/solution deposited Gd_2O_3/sputtered YSZ/sputtered CeO_2.

necessary to fully develop a practical conductor using only solution techniques, but the simplicity and low-cost of this nonvacuum process are major incentives. We are currently investigating other rare-earth oxides, optimization of the processing parameters, solution deposited multilayer buffers, and alternate methods of YBCO deposition.

ACKNOWLEDGMENTS

This work was supported by the United States Department of Energy, Office of Science, Division of Materials Science, and the Office of Energy Efficiency and Renewable Energy and was performed at the Oak Ridge National Laboratory. The Oak Ridge National Laboratory is managed for the United States Department of Energy by the Lockheed Martin Energy Research Corporation under Contract No. DE-AC05-96OR22464.

REFERENCES

1. J.L. MacManus-Driscoll, Annu. Rev. Mater. Sci. **28,** 421 (1998).
2. D. Dimos, P. Chaudhari, and J. Mannhart, Phys. Rev B **41,** 4038 (1990).
3. Y. Iijima, N. Tanabe, and O. Kohno, *Proc. 4th Int. Symp. Supercond. (ISS)* (Springer Verlag, Tokyo, Japan, 1992), p. 679.
4. D.P. Norton, A. Goyal, J.D. Budai, D.K. Christen, D.M. Kroeger, E.D. Specht, Q. He, B. Saffian, M. Paranthaman, C.E. Klabunde, D.F. Lee, B.C. Sales, and F.A. List, Science **274,** 755 (1996).
5. A. Goyal, D.P. Norton, M. Paranthaman, E.D. Specht, D.M. Kroeger, D.K. Christen, Q. He, B. Saffian, F.A. List, D.F. Lee, P.M. Martin, C.E. Klabunde, E. Hartfield, and V.K. Siska, Appl. Phys. Lett. **69,** 1795 (1996).
6. D.P. Norton, C. Park, C. Prouteau, D.K. Christen, M.F. Chisholm, J. D. Budai, S.J. Pennycook, A. Goyal, E.Y. Sun, D.F. Lee, D.M. Kroeger, E. Specht, M. Paranthaman, and N.D. Browning, Mater. Sci. Eng. B-Solid State Mater. Adv. Technol. **56,** 86 (1998).
7. M. Paranthaman, A. Goyal, F.A. List, E.D. Specht, D.F. Lee, P.M. Martin, Q. He, D.K. Christen, D.P. Norton, J.D. Budai, and D.M. Kroeger, Physica C **275,** 266 (1997).
8. D.F. Lee, M. Paranthaman, J.E. Mathis, A. Goyal, D.M. Kroeger, E.D. Specht, R.K. Williams, F.A. List, P.M. Martin, C. Park, D.P. Norton, and D.K. Christen, Jpn. J. Appl. Phys. 2 **38,** L178 (1999).
9. M. Paranathaman, D.F. Lee, A. Goyal, E.D. Specht, P.M. Martin, X. Cui, J.E. Mathis, R. Feenstra, D.K. Christen, and D.M. Kroeger, Supercond. Sci. Technol. **12,** 319 (1999).
10. S.S. Shoup, M. Paranthaman, A. Goyal, E.D. Specht, D.F. Lee, D.M. Kroeger, and D.B. Beach, J. Am. Ceram. Soc. **81,** 3019 (1998).
11. D.B. Beach, C.E. Vallet, M. Paranthaman, E.D. Specht, J.S. Morrell, and Z.B. Xue, in *Chemical Aspects of Electronic Ceramics Processing,* edited by P.N. Kumta, A.F. Hepp, D.B. Beach, B. Arkles, and J.J. Sullivan (Mater. Res. Soc. Symp. Proc. **495,** Warrendale, PA, 1998), p. 263.
12. L.M. Brown and K.S. Mazidiyansi, Inorg. Chem. **9,** 2783 (1990).
13. Powder Diffraction File, Card No. 12-0797, International Center for Diffraction Data.
14. A. Goyal, E.D. Specht, Z.L. Wang, and D.M. Kroeger, Ultramicroscopy **67,** 35 (1997).
15. M. Paranthaman, F.A. List, D.F. Lee, A. Goyal, R. Feenstra, D.P. Norton, C. Park, D.T. Verebelyi, D.K. Christen, P.M. Martin, E.D. Specht, and D.M. Kroeger, in *Science and Engineering of HTC Superconductivity,* Advances in Science and Technology 23, edited by P. Vincenzi (Techna Srl, Faenza, Italy, 1999), p. 185.